Wild-type p53 overexpression in *NPM1*-mutated acute myeloid leukemia: potential implications for disease biology and therapy response

In the latest World Health Organization (WHO) and International Consensus Classification (ICC) diagnostic schema for hematolymphoid neoplasms acute myeloid leukemias (AML) are now largely genetically-defined.[1,2] At seemingly opposite ends of the clinicopathologic and genomic spectra lie AML with mutated *NPM1* (*NPM1*-AML) and AML (and precursor states) harboring *TP53* abnormalities (*TP53*-AML). Approximately 30% of *de novo* AML cases are defined by mutations in *NPM1*, and are commonly associated with a normal karyotype, response to induction therapy, and a relatively favorable clinical course. In contrast, *TP53*-AML are characterized by aneuploidy, uniformly poor response to standard-of-care therapeutic strategies, and a dismal prognosis.

Sequencing studies involving large AML cohorts have revealed *NPM1* and *TP53* mutations to be essentially mutually exclusive.[3-5] In our diagnostic hematopathology practice, we commonly utilize antibody-based immunohistochemistry for mutant NPM1 and p53 proteins as surrogate markers for their underlying genetic lesions as part of the initial examination of AML bone marrow biopsy tissues.[6-9] While moderate to strong p53 staining in a significant proportion of tumor cells (i.e., aberrant accumulation of mutant protein) is highly suggestive of a missense mutation in the *TP53* DNA binding domain, we encountered a similar pattern in several *NPM1*-AML confirmed to be *TP53*-wild type (WT) by sequencing studies. Therefore, we sought to explore the frequency of this protein expression pattern, to identify possible mechanisms for WT p53 overexpression in *NPM1*-AML, and to assess for WT p53 pathway activity in this relatively common AML subtype. This study was performed with Institutional Review Board approval and in accordance with the Declaration of Helsinki.

We analyzed RNA-sequencing data from the Beat AML cohort,[5] filtering cases to include initial diagnosis only, and applied limma (RRID:SCR_010943) to CPM values for differential expression, and to regress differences in sample site and response.[10] Gene set enrichment analysis (GSEA) was performed on the regressed log2 fold change (FC) data using MSigDB signatures.[11] Separately, chromatin immunoprecipitation (ChIP) bigwig files with and without degron treatment were downloaded from GSE197387, a dataset generated as part of a study of NPM1 mutant protein binding to chromatin. The *TP53* locus was visualized by IGV, but there was no discernable difference based on *NPM1* degron treatment (i.e., no evidence of mutant *NPM1* activity at the *TP53* promoter).

In select cases of molecularly-confirmed *NPM1*-mutated/*TP53*-WT AML, we have observed p53 expression approaching the level often found in other cases harboring missense mutations in the DNA binding domain of *TP53* (Figure 1A, representative case). Based on an analysis of the BeatAML cohort dataset,[5] we found that *NPM1*-AML cases (N=74) are associated with significantly higher *TP53* expression than *TP53*-WT/*NPM1*-WT cases (N=190) (P=0.047, multivariate limma model) (Figure 1B). We considered the possibility that this difference may be driven by other prognostically-significant mutations co-occurring with *NPM1* (*FLT3*-internal tandem duplication [ITD], *FLT3*-tyrosine kinase domain [TKD], *DNMT3A, SF3B1, SRSF2, U2AF1*); however, exclusion of these genes by comparing cases of *NPM1*-AML to *NPM1*-WT/*TP53*-WT/gene mutation-positive cases revealed a similar result (P=0.018, multivariate limma model) (Figure 1C). Furthermore, we observed no effect of specimen type (e.g., peripheral blood, bone marrow, or leukapheresis product) on *TP53* expression level (Figure 1D).

To assess the activity of WT-p53 signaling we focused on known p53-associated gene sets. By comparing *NPM1*-AML with *TP53*-AML cases (N=17), we first established the pattern of up-/down-regulation for gene sets associated with DNA repair, apoptosis, and cell cycle pathways as a function of *TP53* mutation (Figure 1E). Despite the genetic heterogeneity among *NPM1*-WT cases, relative to *NPM1*-AML cases the -WT group exhibited a similar gene set enrichment pattern as seen for *TP53*-AML cases (Figure 1F). We next performed a similar analysis restricted only to *NPM1*-AML cases, comparing the uppermost (N=19) and lowermost (N=19) quartiles for *TP53* gene expression; we noted a partial overlap in the pattern of up- and/or downregulation across DNA repair, apoptosis, and cell cycle gene sets as we observed when comparing *NPM1*-AML and *TP53*-AML cases (Figure 1G), suggesting that the activity of these pathways may be directly influenced by WT-p53 dosage within the context of *NPM1*-AML.

Additionally, archival (paraffin-embedded) bone marrow aspirate specimens, originally collected for routine diagnostic evaluation of suspected leukemia at Weill Cornell Medical College/NewYork-Presbyterian Hospital (WCM/NYP), were used. A total of 45 leukemia patient samples were studied, including *NPM1*-mutated AML (N=33) (Table 1), *TP53*-mutated AML (N=5), and *NPM1*/*TP53*-WT AML with normal karyotype (N=7). Clinical and laboratory data were also collected. Cytogenetic and next-generation sequencing data for all cases were generated and collect-

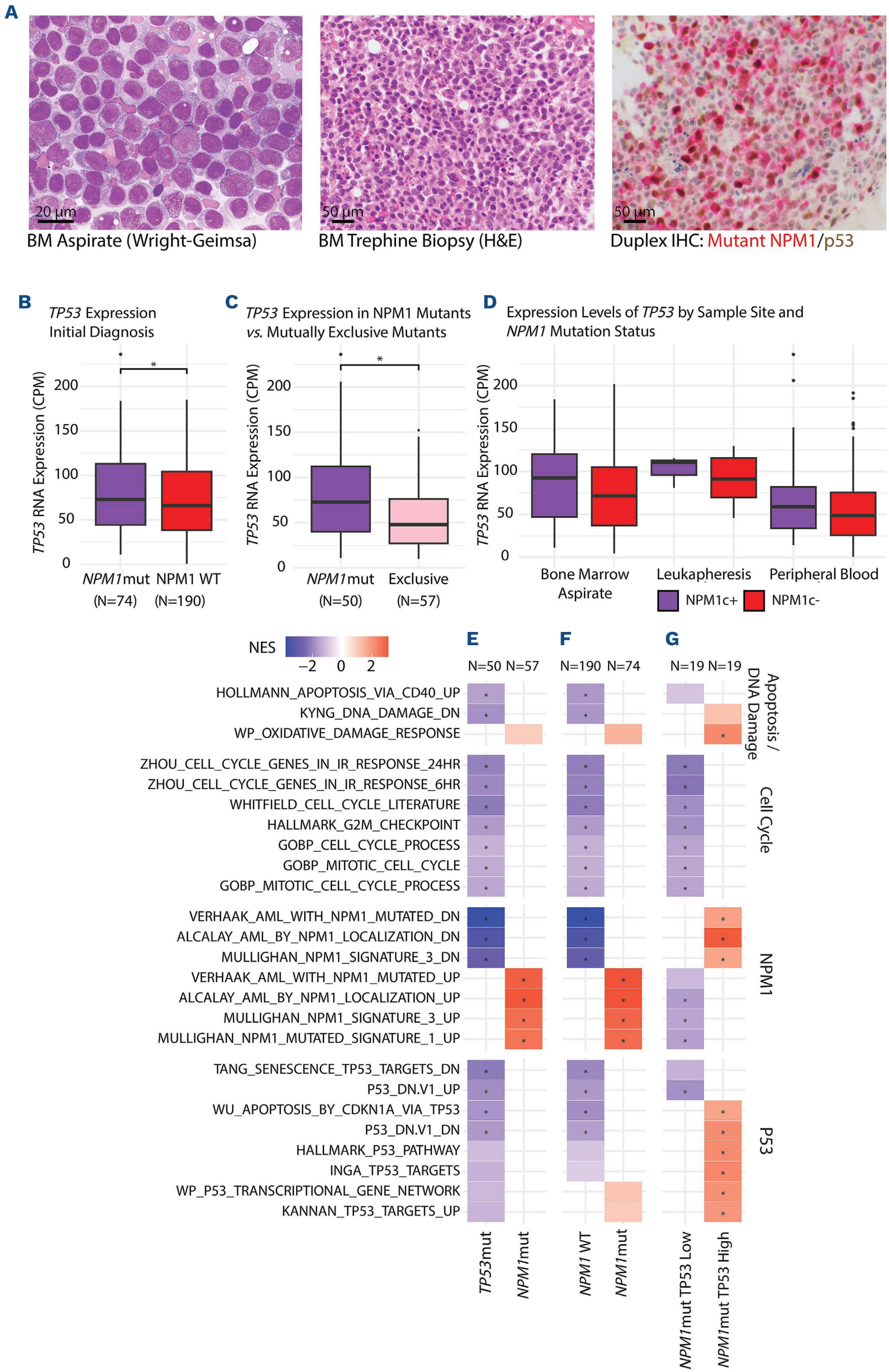

Continued on following page.

Figure 1. *TP53* is over-expressed in *NPM1*-acute myeloid leukemia relative to other acute myeloid leukemia and associated with p53 pathway activity. (A) Representative case of *NPM1* acute myeloid leukemia (*NPM1*-AML). Bone marrow (BM) aspirate smear preparation shows a predominance of blasts with monocytic features (top left, Wright-Giemsa, 1,000x). Histologic evaluation of the trephine biopsy shows sheets of medium to large sized blasts with monocytic features (top right, hematoxylin and eosin, 600x). Duplex chromogenic immunohistochemistry for p53 (brown) and mutant NPM1 (red) proteins reveals frequent moderate to strong p53 expression in mutant NPM1-positive cells (bottom, p53 (DAB)/mutant NPM1 (Fast Red), 600x). (B) *TP53* is more highly expressed in *NPM1*-AML compared to *NPM1*-wild-type (WT) AML cases (*P*=0.047, multivariate limma model). (C) Among *NPM1*-AML cases, *TP53* is more highly expressed in those lacking co-mutation in *DNMT3A, FLT3, SF3B1, SRSF2, U2AF1* (*P*=0.018, multivariate limma model). (D) *TP53* is more highly expressed in *NPM1*-AML compared to *NPM1*-WT AML, irrespective of sample type; statistical analysis was performed as part of panel (B) data. (E-G) Gene set enrichment analyses (GSEA) of msigdb pathways colored by normalized enrichment score (NES), with significance (*P* adjusted <0.05) denoted by an asterisk. p53-mediated pathways related to DNA repair, apoptosis, and cell cycle are more active in *NPM1*-AML relative to *TP53*-AML (E), and several are more active in *NPM1*-AML compared to *NPM1*-WT/TP53-WT AML (F). Among *NPM1*-AML, statistically significant pathway differences are observed between cases in the uppermost *versus* lowermost quartiles for *TP53* co-expression; those in the lowermost quartile exhibit pathway enrichment partially overlapping that observed for *TP53*-mutated cases (G).

ed as previously described;[8] all cases were assessed for *NPM1* and *TP53* coding sequence mutations. Multiplexed immunofluorescence (MxIF) was performed using the Opal system (Akoya Biosciences, Marlborough, MA) by staining 4 micron-thick formalin-fixed, paraffin-embedded aspirate fluid ("clot sections") as described previously.[12] Antibodies were selected from a menu of extensively validated and clinically tested clones in our CLIA laboratory (Weill Cornell Medicine/NewYork-Presbyterian Hospital, New York, NY).

Whole slide MxIF images were captured using the Phenoimager platform (Akoya Biosciences) and analyzed in HALO (v3.6.4134.95, Indica Labs, Albuquerque, NM) by two hematopathologists (PB and SSP). We phenotyped cells *in situ* at single cell resolution, identifying them as *NPM1*-mutant or -WT using a mutant protein-specific antibody, and then evaluated the frequency and intensity of p53 expression (Figure 2A). Single cell count matrices were output and further analyzed in R v.4.4.1 (RStudio version 2023.06.1 Build 524). Wilcoxon signed rank exact test was used to compare the proportions of positive p53 expression and mean fluorescence intensity in *NPM1* mutant *versus* WT cells, as well as the proportions of p53 expression in *NPM1*-mutated cells between complete remission with or without complete count recovery (CR/CRi) and persistent disease (PD) groups. *P* value <0.05 was considered statistically significant. The same *P* value was used to assess differential gene expression; no adjustment was performed as only *TP53* values were assessed.

The median number of nucleated cells analyzed per case was 8,957 (range, 1,869-31,151) (*Online Supplementary Figure S1*). Within each case, a greater proportion of *NPM1*-mutated cells were p53-positive, compared to *NPM1*-WT cells (*P*<0.001, paired Wilcoxon test) (Figure 2B; *Online Supplementary Figure S3*); overall, we found >10% of NPM1-mutant cells to be p53-positive in 24 of 33 cases (73%). Similarly, the mean fluorescence intensity (MFI) of p53 was higher in *NPM1*-mutant compared to WT cells (P<0.001, paired Wilcoxon test) (Figure 2C; *Online Supplementary Figure S3*). We observed no significant difference in p53 proportion between patients above or below the age of 60, in those presenting with or without leukocytosis, or with respect to peripheral blood or bone marrow blast percentage (*data not shown)*. We considered the possibility that p53 expression may simply be associated with a non-G0 state of the leukemic cells; however, we observed no correlation between p53 and Ki67 expression (*Online Supplementary Figure S2A*). We also wondered if p53 overexpression could be a result of diminished MDM2-mediated degradation due to cytoplasmic sequestration of MDM2 by mutant NPM1; however, an analysis of the few highest p53 co-expressors revealed no significant cytoplasmic MDM2 signal by MxIF (*Online Supplemental Figure S2B*). Furthermore, we found no significant difference in p53 co-expression frequency based on presence or absence of common co-mutations (e.g., *FLT3*-ITD, *DNMT3A*, *IDH1/2*) (*Online Supplementary Figure S2C*). As a proportion of total nucleated cells, p53 was most frequently detected in *TP53*-AML cases, as anticipated; *NPM1*-AML cases included a range of p53 expression frequency, with a subset exhibiting p53 expression near the level found in *TP53*-AML cases. We observed no significant difference in p53 co-expression among total nucleated cells between *NPM1*-AML and a small comparison group of normal karyotype *NPM1*-WT cases (*P*>0.05) (Figure 2D). Similarly, p53 MFI was significantly higher in *TP53*-mutated *versus* all *TP53*-WT cases (Figure 2E).

Post-induction remission status was available for 27 of the 33 cases analyzed. Interestingly, we found a significantly higher p53-positive proportion among *NPM1*-mutated cells at diagnosis in patients who achieved complete remission with or without complete count recovery (CR/CRi, N=21) compared to patients with grossly persistent disease (PD, N=6) (median 0.219 *vs*. 0.086; *P*=0.018) (Figure 2F). Of note, we found no difference in the frequency of *FLT3*-ITD co-mutations in CR/CRi *versus* PD patients (*P*>0.05).

In this study, we observed higher *TP53* gene expression in *NPM1*-AML cases compared to *NPM1*-WT AML cases. Given recently published data demonstrating that mutant NPM1 protein directly binds to chromatin to modify gene expression,[13,14] we explored the possibility that mutant NPM1 could be directly driving *TP53* expression, but did not find compelling evidence to support this mechanism. Using GSEA, we observed an overlapping pattern of positively or

Table 1. Clinicopathologic features and p53 co-expression measurements for primary *NPM1*-AML tissue samples.

Case #	M/F	Age, years	WBC, x10⁹/L	Hb, g/dL	Plt, x10⁹/L	BM blast %	PB blast %	Karyotype	*NPM1* VAF	p53+ of NPM1c⁺	Co-mutations (Tiers I & II)	*FLT3*-ITD	Induction	CR/CRi/PD
NPM1c-1	F	37	1.2	8.0	52.0	25	0.0	NK	N/A	0.30	N/A	N	7+3	CR
NPM1c-2	M	60	73.0	11.3	103.0	84	65.0	47,XY,+8[1]/46,XY[19]	N/A	0.81	N/A	N/A	7+3	CRi
NPM1c-3	F	65	2.9	9.3	81.0	51	1.0	NK	N/A	0.12	*DNMT3A, TET2*	N	7+3	CR
NPM1c-4	M	64	30.8	10.1	94.0	24	43.0	46,XY,inv(9)(p12q13)c[20]	N/A	0.09	None	Y	7+3	PD
NPM1c-5	M	26	89.9	9.8	13.0	69	69.0	NK	N/A	0.11	*DNMT3A, FLT3*-TKD	N	7+3	CR
NPM1c-6	F	37	44.0	6.6	56.0	85	97.0	NK	N/A	0.43	*IDH1, FLT3*-TKD	N	7+3	CR
NPM1c-7	F	50	17.4	10.3	50.0	89	59.0	NK	0.560	0.13	None	Y	7+3	CR
NPM1c-8	F	74	44.0	8.8	27.0	96	92.0	NK	0.440	0.17	*DNMT3A, TET2*	Y	N/A	N/A
NPM1c-9	F	56	23.3	9.5	71.0	86	90.0	NK	0.460	0.38	*IDH1*	Y	7+3	CR
NPM1c-10	F	94	N/A	N/A	N/A	53	4.0	NK	0.280	0.11	*DNMT3A, TET2, SF3B1*	Y	Decitabine	PD
NPM1c-11	F	73	18.0	8.3	92.0	75	7.0	NK	0.400	0.06	*DNMT3A, TET2*	N	LDAC/Ven	PD
NPM1c-12	M	63	74.3	7.8	36.0	88	90.0	NK	0.510	0.13	*DNMT3A, PTPN11, NF1*	N	N/A	N/A
NPM1c-13	M	51	39.8	7.3	42.0	53	29.0	NK	0.500	0.24	*DNMT3A, NRAS*	Y	7+3	CR
NPM1c-14	F	45	16.0	7.5	361.0	65	14.0	NK	0.420	0.07	*DNMT3A, CEBPA*	N	7+3	CR
NPM1c-15	F	42	73.2	10.1	64.0	90	80.0	NK	0.460	0.49	*DNMT3A*	Y	7+3 plus midostaurin	CR
NPM1c-16	M	85	9.6	8.7	45.0	88	89.0	NK	0.360	0.06	*DNMT3A, IDH1*	N	N/A	N/A
NPM1c-17	M	62	75.5	12.4	40.0	86	80.0	47,XY,+8[13]/46,XY[2]	0.450	0.55	*DNMT3A, ASXL1, FLT3-TKD*	N	7+3	CR
NPM1c-18	F	56	22.6	9.9	23.0	93	94.0	NK	0.640	0.43	*DNMT3A, TET2*	Y	7+3	CR
NPM1c-19	M	56	6.8	7.9	72.0	83	71.0	NK	0.470	0.22	*DNMT3A, IDH2, ZRSR2*	N	7+3	CR
NPM1c-20	M	67	120.3	8.6	22.0	98	98.0	NK	0.540	0.20	*IDH2, SRSF2, FLT3*-TKD	N	N/A	N/A
NPM1c-21	F	70	27.0	10.9	122.0	44	50.0	NK	0.370	0.14	*DNMT3A, IDH1*	N	Decitabine	PD
NPM1c-22	M	72	1.0	9.2	28.0	73	5.0	48,XY,+8,+8[20]	0.170	0.45	*DNMT3A, NF1, NRAS*	N	CPX-351	CR

Continued on following page.

Case #	M/F	Age, years	WBC, x10⁹/L	Hb, g/dL	Plt, x10⁹/L	BM blast %	PB blast %	Karyotype	*NPM1* VAF	p53+ of NPM1c⁺	Co-mutations (Tiers I & II)	*FLT3*-ITD	Induction	CR/CRi/ PD
NPM1c-23	F	58	313.8	8.5	36.0	97	95.0	NK	0.580	0.36	*TET2*, *FLT3*-TKD	N	N/A	N/A
NPM1c-24	F	61	2.8	11.5	122.0	88	65.0	NK	0.430	0.15	*DNMT3A, IDH1*	N	CPX-351	CR
NPM1c-25	M	69	21.0	10.5	123.0	70	2.0	NK	0.340	0.27	*TET2, PTPN11, IDH1*	N	N/A	N/A
NPM1c-26	F	77	90.5	6.3	33.0	70	82.0	NK	0.440	0.27	None	Y	Aza/Ven	CRi
NPM1c-27	F	57	1.1	8.5	42.0	70	27.0	NK	0.190	0.07	*IDH1*	N	7+3	CR
NPM1c-28	M	58	12.4	6.5	25.0	33	9.0	45,X,-Y[11]/46,XY[9]	0.460	0.03	*DNMT3A*	N	7+3	PD
NPM1c-29	F	58	14.2	11.1	30.0	30	45.0	NK	0.399	0.12	*NRAS, IDH2*	N	7+3	CR
NPM1c-30	M	47	46.0	8.1	17.0	75	57.0	NK	0.405	0.05	*DNMT3A, FLT3*-TKD	Y	7+3	CR (IHC/ PCR⁺)
NPM1c-31	F	30	3.9	7.3	94.0	70	20.0	NK	0.282	0.16	*DNMT3A, CEBPA, ETV6, SMC1A*	N	N/A	CR (IHC/NGS MRD⁺)
NPM1c-32	M	53	67.3	11.1	70.0	75	48.0	NK	0.427	0.08	*TET2, WT1*	N	PALG trial	PD
NPM1c-33	M	66	1.6	12.9	170.0	57	3.0	NK	0.205	0.02	*NRAS, IDH1, WT1*	N	N/A	CRi (IHC/PCR MRD⁺)

M: male; F: female; WBC: white blood cell count; Hb: hemoglobin concentration; Plt: platelet count; BM: bone marrow; PB:peripheral blood; NK: normal karyotype; VAF: variant allele frequency; NPM1c: mutant NPM1; CR: completion remission; CRi: complete remission with incomplete count recovery; PD: persistent disease (i.e., BM blast >5%); LDAC: low-dose cytarabine; Aza: azacitidine; Ven: venetoclax; PALG, daunorubicin/cytarabine +/- cladribine; IHC: immunohistochemistry, N/A: not available; NGS: next-generation sequencing; PCR: polymerase chain reaction; MRD: minimal/measurable residual disease.

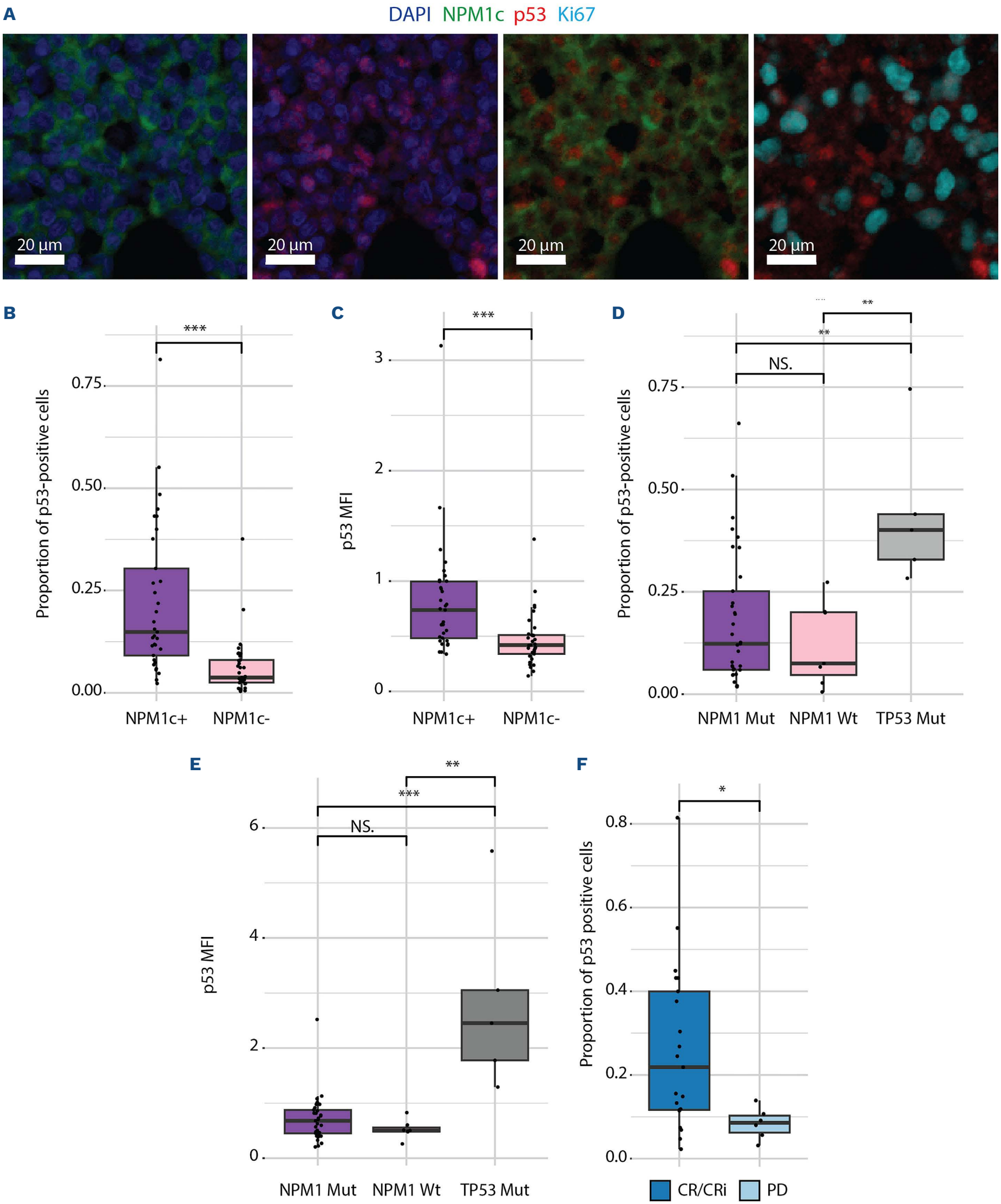

Figure 2. p53 is over-expressed in *NPM1*-mutated cells in primary patient samples and low co-expression correlates with persistent disease post-induction therapy. (A) Representative mutiplexed immunofluorescence (MxIF) images from a case of NPM1 acute myeloid leukemia (*NPM1*-AML) labeled with visualization of nuclei (DAPI), mutant NPM1 [NPM1c] (green), p53 (red), and Ki67

Continued on following page.

(cyan). Mutant NPM1-positive cells exhibit frequent nuclear co-expression of p53. Frequent p53 and Ki67 co-expression is not observed (see *Online Supplementary Figure S2*). (B, C) Within each case of *NPM1*-AML analyzed by MxIF, a greater proportion of *NPM1*-mutated cells are p53-positive (B) and demonstrate higher p53 mean fluorescent intensity (C), compared to *NPM1*-wild-type (WT) cells (P<0.001, paired Wilcoxon tests). (D, E) *TP53*-AML cases (N=5) have the highest proportion of p53-positive cells (D), as well as highest p53 mean fluoresesence intensity (MFI) (E), among all nucleated cells analyzed. No significant difference in frequency of p53 expression or p53 MFI among total cells between *NPM1*-AML (N=33) and *TP53/NPM1*-WT AML cases with normal karyotype (N=7). (F) Higher p53-positive proportion among NPM1-mutated cells at diagnosis in patients who achieved complete remission with or without complete count recovery (CR/CRi, N=21) post-induction compared to patients with persistent disease (PD, N=6) (median 0.219 *vs*. 0.086; P=0.018). NS: not significant.

negatively enriched gene sets for *NPM1*-AML cases when compared to either *TP53*-AML or *NPM1*-WT cases. Interestingly, separating *NPM1*-AML cases into those with high and low *TP53* co-expression recapitulated the gene set enrichment differences observed between *NPM1*-AML and *TP53*-AML cases, suggesting that low *TP53* co-expression in *NPM1*-AML may approximate the absence of a normally functioning p53 protein.

Finally, by applying MxIF staining to primary patient samples coupled with single cell resolution-based digital image analysis, we discovered elevated p53 expression in >10% of *NPM1*-mutant cells in 73% of the analyzed cases, with a higher frequency and intensity of p53 expression in *NPM1* mutant relative to WT cells observed in all cases. Interestingly, patients with grossly persistent disease following induction therapy were characterized by a significantly lower frequency of p53 expression at diagnosis than those who achieved complete remission. Low-plex multiparametric tissue imaging, as employed in this study, also has potential utility in the routine clinical diagnostic setting; particularly in hematolymphoid neoplasms, including a broad range of leukemias and lymphomas, where cellular composition is often heterogeneous and more precise evaluation and quantification of biomarkers in specific cell subsets may provide additional prognostic and/or predictive value. Importantly, this method involves automated tissue staining, as is routinely performed in clinical immunohistochemistry laboratories, accompanied by an automated whole slide imaging and biomarker quantification workflow driven by commercially-available software packages; therefore, it is feasible to interrogate for WT-p53 expression in routine treatment-naïve cases of *NPM1*-AML, with data typically available within 24 hours. Although validation of this biomarker in a larger prospective clinical cohort will be required, it may be feasible to define an optimal threshold for classifying patients as low or high WT-p53 co-expressors, and thereby identify patients at diagnosis who are more likely to experience primary refractory disease. The same basic protocols and analytical workflow can consequently be implemented in more than one laboratory.

Our study is limited by its retrospective design, the small internal cohort of patient samples studied, and largely correlative findings. However, to the best of our knowledge, our data provide the first evidence that many *NPM1*-AML cases are characterized by elevated *TP53* gene and p53 protein expression at baseline and associated with activity of p53-mediated gene expression pathways linked to DNA repair, apoptosis, and cell cycle regulation opposite that observed in *TP53*-AML. It remains possible that this profile could be driven by either (i) MDM2 sequestration by residual WT-NPM1 protein with consequently reduced MDM2-mediated p53 degradation, or (ii) p53 stabilization via phosphorylation at select serine residues.[15] Nonetheless, we hypothesize that while increased WT-p53 activity might contribute to the intrinsic biological and clinical features of most *NPM1*-AML cases, low WT-p53 co-expression in a subset of cases at diagnosis could represent a potential biomarker of unfavorable disease worthy of further exploration in larger cohorts.

Authors

Paul D. Barone,[1*] Siarhei Dzedzik,[2*] Ashley S. Kleinman,[3-5*] Christopher R. Chin,[4,6,7] Cem Meydan,[3,4,6] Itzel Valencia,[8] Mayumi Sugita,[9] Monica L. Guzman,[9] Joshua A. Fein,[9] Justin D. Kaner,[9] Pinkal Desai,[9] Gail J. Roboz,[9] Ari M. Melnick,[9] Christopher E. Mason[3,4,6,7,10,11] and Sanjay S. Patel[1,8]

[1]Division of Hematopathology, Department of Pathology and Laboratory Medicine, Weill Cornell Medicine/NewYork-Presbyterian Hospital, New York, NY; [2]Department of Pathology and Laboratory Medicine, Weill Cornell Medicine/NewYork-Presbyterian Hospital, New York, NY; [3]Department of Physiology and Biophysics, Weill Cornell Medicine, New York, NY; [4]The HRH Prince Alwaleed Bin Talal Bin Abdulaziz Alsaud Institute for Computational Biomedicine, Weill Cornell Medicine, New York, NY; [5]Department of Earth, Atmospheric, and Planetary Sciences, Massachusetts Institute of Technology, Cambridge, MA; [6]Department of Medicine, Weill Cornell Medicine, New York, NY; [7]Tri-Institutional Computational Biology and Medicine Program, Weill Cornell Medicine, New York, NY; [8]Multiparametric In Situ Imaging (MISI) Laboratory, Department of Pathology and Laboratory Medicine, Weill Cornell Medicine, New York, NY; [9]Division of Hematology and Medical Oncology, Department of Medicine, Weill Cornell Medicine/New York-Presbyterian Hospital, New York, NY; [10]The Feil Family Brain and Mind Research Institute, Weill Cornell Medicine, New York, NY and [11]WorldQuant Initiative for Quantitative Prediction, Weill Cornell Medicine, New York, NY, USA

**PDB, SD and ASK contributed equally as first authors.*

Correspondence:
S.S. PATEL - sap9151@med.cornell.edu

https://doi.org/10.3324/haematol.2025.288054

Received: April 28, 2025.
Accepted: September 2, 2025.
Early view: September 11, 2025.

Disclosures
No conflicts of interest to disclose.

Contributions
Experiments were designed, executed and/or analyzed by PB, IV, ASK, CRC, CM, MG, JK, JAF, AM, CEM, and SSP. IV performed multiplex tissue staining and imaging. JK, JAF, GJR and PD reviewed clinical data. The manuscript was written by PB and SSP with input from all authors. PB and SSP conceived of and designed the study. SSP supervised the work.

Acknowledgments
The authors thank the Weill Cornell Medicine Department of Pathology and Laboratory Medicine's Center for Translational Pathology (CTP) and Multiparametric *In Situ* Imaging (MISI) Laboratory.

Funding
This work was supported by the Department of Pathology and Laboratory Medicine, Weill Cornell Medical College (start-up funding to SSP). CRC is supported by an NIH post-doctoral training grant (T32AR071302).

Data-sharing statement
Analysis code and data are available at https://github.com/cmason-lab. Any additional requests can be submitted in writing via e-mail to the to the corresponding author.

References

1. Khoury JD, Solary E, Abla O, et al. The 5th edition of the World Health Organization Classification of Haematolymphoid Tumours: myeloid and histiocytic/dendritic neoplasms. Leukemia. 2022;36(7):1703-1719.
2. Arber DA, Orazi A, Hasserjian RP, et al. International Consensus Classification of Myeloid Neoplasms and Acute Leukemias: integrating morphologic, clinical, and genomic data. Blood. 2022;140(11):1200-1228.
3. Othman J, Potter N, Ivey A, et al. Molecular, clinical, and therapeutic determinants of outcome in NPM1-mutated AML. Blood. 2024;144(7):714-728.
4. Papaemmanuil E, Gerstung M, Bullinger L, et al. Genomic classification and prognosis in acute myeloid leukemia. N Engl J Med. 2016;374(23):2209-2221.
5. Tyner JW, Tognon CE, Bottomly D, et al. Functional genomic landscape of acute myeloid leukaemia. Nature. 2018;562(7728):526-531.
6. Pasqualucci L, Liso A, Martelli MP, et al. Mutated nucleophosmin detects clonal multilineage involvement in acute myeloid leukemia: Impact on WHO classification. Blood. 2006;108(13):4146-4155.
7. Patel SS, Pinkus GS, Ritterhouse LL, et al. High NPM1 mutant allele burden at diagnosis correlates with minimal residual disease at first remission in de novo acute myeloid leukemia. Am J Hematol. 2019;94(8):921-928.
8. Lopez A, Patel S, Geyer JT, et al. Comparison of multiple clinical testing modalities for assessment of NPM1-mutant AML. Front Oncol. 2021;11:701318.
9. Tashakori M, Kadia T, Loghavi S, et al. TP53 copy number and protein expression inform mutation status across risk categories in acute myeloid leukemia. Blood. 2022;140(1):58-72.
10. Ritchie ME, Phipson B, Wu D, et al. limma powers differential expression analyses for RNA-sequencing and microarray studies. Nucleic Acids Res. 2015;43(7):e47.
11. Subramanian A, Tamayo P, Mootha VK, et al. Gene set enrichment analysis: a knowledge-based approach for interpreting genome-wide expression profiles. Proc Natl Acad Sci U S A. 2005;102(43):15545-15550.
12. Sarachakov A, Varlamova A, Svelolkin V, et al. Spatial mapping of human hematopoiesis at single cell resolution reveals aging-associated topographic remodeling. Blood. 2023;142(26):2282-2295.
13. Uckelmann HJ, Haarer EL, Takeda R, et al. Mutant NPM1 directly regulates oncogenic transcription in acute myeloid leukemia. Cancer Discov. 2022;13(3):746-765.
14. Wang XQD, Fan D, Han Q, et al. Mutant NPM1 hijacks transcriptional hubs to maintain pathogenic gene programs in acute myeloid leukemia. Cancer Discov. 2023;13(3):724-745.
15. Ashcroft M, Kubbutat MH, Vousden KH. Regulation of p53 function and stability by phosphorylation. Mol. Cell Biol. 1999;19(3):1751-1758.